Atmósfera 20(4), 341-358 (2007)

The global and UV-B radiation over Egypt

H. A. BASSET
Department of Astronomy and Meteorology, Faculty of Science,
Al-Azhar University, Cairo, Egypt
Corresponding author; e-mail: heshmatm@yahoo.com

M. H. KORANY
Egyptian Meteorological Authority, Cairo, Egypt

Received February 20, 2006; accepted January 25, 2007

RESUMEN

En este trabajo se estudia la relación entre la radiación UV-B y la radiación global sobre Egipto. Se investigan las relaciones entre la radiación solar global y la radiación UV-B y se deducen formulas lineales empíricas para determinar la radiación UV-B a partir de la radiación solar global. Utilizando los registros de radiación solar global en estaciones donde no hay mediciones de UV-B se obtiene ésta utilizando las ecuaciones deducidas. Debido a las variaciones en la periodicidad de la radiación solar, global y UV-B, los valores adimensionales se expanden en series de Fourier. Los coeficientes de Fourier se determinan utilizando los datos de radiación solar global medida en estaciones seleccionadas. Estos coeficientes se utilizan para calcular la radiación UV-B con base en la radiación solar global de las mismas estaciones. Se presenta una comparación entre la radiación UV-B observada y calculada obtenida a partir de los dos métodos de estimación. La comparación muestra un buen acuerdo entre la radiación UV-B observada y calculada. La aplicación del método de regresión lineal para calcular la radiación UV-B en estaciones donde no hay mediciones de ésta es mejor que el método de coeficientes de Fourier.

ABSTRACT

This work studies the relation between UV-B radiation and global radiation over Egypt. The relationships between the global solar radiation and UV-B radiation at four stations in Egypt have been studied, and linear empirical formulas for estimating UV-B from global radiation at these stations has been deduced. The deduced equations were applied to calculate the UV-B radiation for other stations where measurements were unavailable, using records of global radiation at these stations. Because of the periodicity of variations in solar radiation, global and UV-B radiation, the non-dimensional values are expanded in Fourier series. Fourier coefficients were determined by using measured global solar radiation data of the selected stations. These coefficients were used to calculate UV-B radiation based on global solar radiation for the same stations. A comparison between observed and calculated UV-B radiation arising from the two methods of estimation is presented. The comparison showed a good agreement between the observed and estimated UV-B radiation. The application of linear regression method to calculate solar radiation for other stations where UV-B radiation measurements were unavailable was better than Fourier coefficients method.

Keywords: UV-B radiation, global radiation, empirical equations, harmonic analysis, monthly variations.

1. Introduction

During the last years, concerns about the intensity levels of UV-B radiation reaching the ground have increased due to the stratospheric ozone depletion and the dramatic increase in the number of skin cancers in the population. The UV solar irradiance at the ground varies greatly with local time, latitude and season, primarily because of the changing elevation of the sun in the sky (Frederick and Carynelisa, 1994). Solar UV radiation, which comprises 8.73% (ASTM, 1981) of the exoatmospheric solar spectrum, consists of three wavelength band-regions, the UV-A (315-400 nm), the UV-B (280-315 nm) and the UV-C (<290 nm), accounting for 5.9, 1.33 (Iqbal,1983) and 1.5% respectively. The Earth's atmosphere significantly modifies the incoming solar radiation through the absorption and scattering process by gases, dust particles and other biosphere constituents of human and natural activities. There is clear linear correlation between UV-total and global solar radiation, particularly in the region of moderate to low global solar radiation values (Koronakis *et al*., 2002). A good linear relationship exists between the UV-B and global irradiance, which enables estimation of UV-B flux in tropical/equatorial areas where facilities for UV-B measurements are not available, but global radiation flux data exist (Ilyas *et al.,* 1999).

The purpose of this paper is to study the relationships between the global solar radiation and UV-B radiation at four stations in Egypt, then deducing empirical formulas for estimating UV-B from global radiation at these stations. The deduced equations are applied to calculate the UV-B radiation for other stations where UV-B radiation measurements are unavailable, using records of global radiation at these stations. Also we used the above results to illustrate the monthly pattern of UV-B over Egypt. Because of the periodicity in the variation of global solar radiation and UV-B radiation data, we made a harmonic analysis for the erythemal exposure UV-B data. Their non-dimensional values were expanded in Fourier series. Fourier coefficients were determined by using measured global solar radiation data of the selected Egyptian weather stations. These coefficients were used to calculate UV-B radiation based on global solar radiation for the same stations. Finally, the comparison between the two methods of estimation was held using Rafah and South Valley stations.

2. Data and measurements

The basic solar radiation network includes fourteen stations whose geographical locations and their items are shown in Table I. They were arranged according to latitude from south to north, and so they represent the different climates of Egypt. Five of them are coastal, namely Sidi Barani, Mersa Matruh, El-Arish and Rafah which are located on the Mediterranean Sea coast, while Hurghada is located on the Red Sea Coast. The other stations are El-Tahrir, Bahtim, Cairo, Malawy, Asyut, South Valley and Aswan, which can be defined as urban sites located in the river Nile valley. The last two stations are located along the western desert of Egypt.

The first measurements of UV-B radiation occurred at Hurghada starting in January 1994. The measurements at El-Arish, started in April 1998. While at Aswan, south of Egypt the measurements started in August 1998. The fourth station was South Valley, in the Upper Egypt, its measurements started in April 2000. The last station was Rafah, about 45 kilometers east of El-Arish station, its measurements started in June 2000. Global solar radiation, diffusive solar radiation and sunshine duration were measured on all these locations simultaneously.

Table I. Egyptian radiation stations network.

Station	WMO No.	Lon. (°E)	Lat. (°N)	Alt. (m)	Global	Diffuse	Direct	UV	UV-B
Aswan	414	32.78	23.97	192	M	M	M	M	M
South Valley	402	32.7	26.16	77.3	M	M	M	M	M
El-Kharga	435	30.53	25.45	78	M	M	- - -	- - -	- - -
Asyut	392	31.02	27.05	5	M	M	- - -	- - -	- - -
Hurghada	464	33.75	27.283	6.5	M	M	- - -	- - -	M
Malawy	389	30.75	27.7	44.3	M	M	- - -	- - -	- - -
Cairo	370	31.28	30.08	36	M	M	- - -	- - -	- - -
Bahtim	369	31.25	30.13	17	M	M	- - -	- - -	- - -
El-Tahrir	345	30.7	30.65	19	M	M	- - -	- - -	- - -
Wadi El-Natron	357	30.37	30.4	49.98	M	M	- - -	- - -	- - -
El-Arish	336	33.83	31.08	32	M	M	M	M	M
Rafah	335	34.2	31.22	73	M	M	M	M	M
Mersa Matruh	306	27.17	31.52	38	M	M	- - -	- - -	- - -
Sidi Barrani	301	25.9	31.62	27	M	M	- - -	- - -	- - -

M: The station measures this item; - - -: the station does not measure this item

3. The relationship between global and UV-B radiation

Here we present the behavior of total global solar irradiation (G) and UV-B radiation for a period of about two years and a half of continuous measurements. These periods of measurements of daily UV-B have been analyzed to illustrate whether any systematic relationship exists between the two variables. Figure 1a presents the daily values of G and UV-B radiation for El Arish. It shows that the maximum values of G and UV-B radiation occur in the summer months with the greatest values at June. While the minimum values occurs in the winter months with the lowest values at January. Generally, it is clear that the annual wave is the dominant wave on the variation of global and UV-B radiation during the year. Also it can be noticed that the higher variability of the values of G and UV-B radiation throughout the year was due to the influence of cloud variability during the year. Figure 1b illustrates the values of G and UV-B for Hurghada during the period from January 1994 to April 1996. The maximum values also occur in the summer season while the minimum values occur in winter. The maximum variability of the values of G and UV-B appears during the spring and winter seasons as a result of high changes in cloud cover over the station during these seasons. Figure 1c illustrates the values of G and UV-B of South Valley during the period from April 2000 to September 2001. Also as in the first two stations, the maximum values occur during summer while the minimum values occur during winter. The measurements of solar radiation at this station are influenced by the sand and dust storms especially during the spring and summer seasons. The values of G and UV-B at Aswan for the period from August 1998 to November 2000 are presented in Figure 1d. The influence of sand and dust storms during the spring and the beginning of summer seasons can be seen in the measurements of G and UV-B. Also there are some cases of rising sand occurring in winter as a characteristic of Aswan weather. The above analyses illustrate that there is a strong correlation between G and UV-B at the four stations.

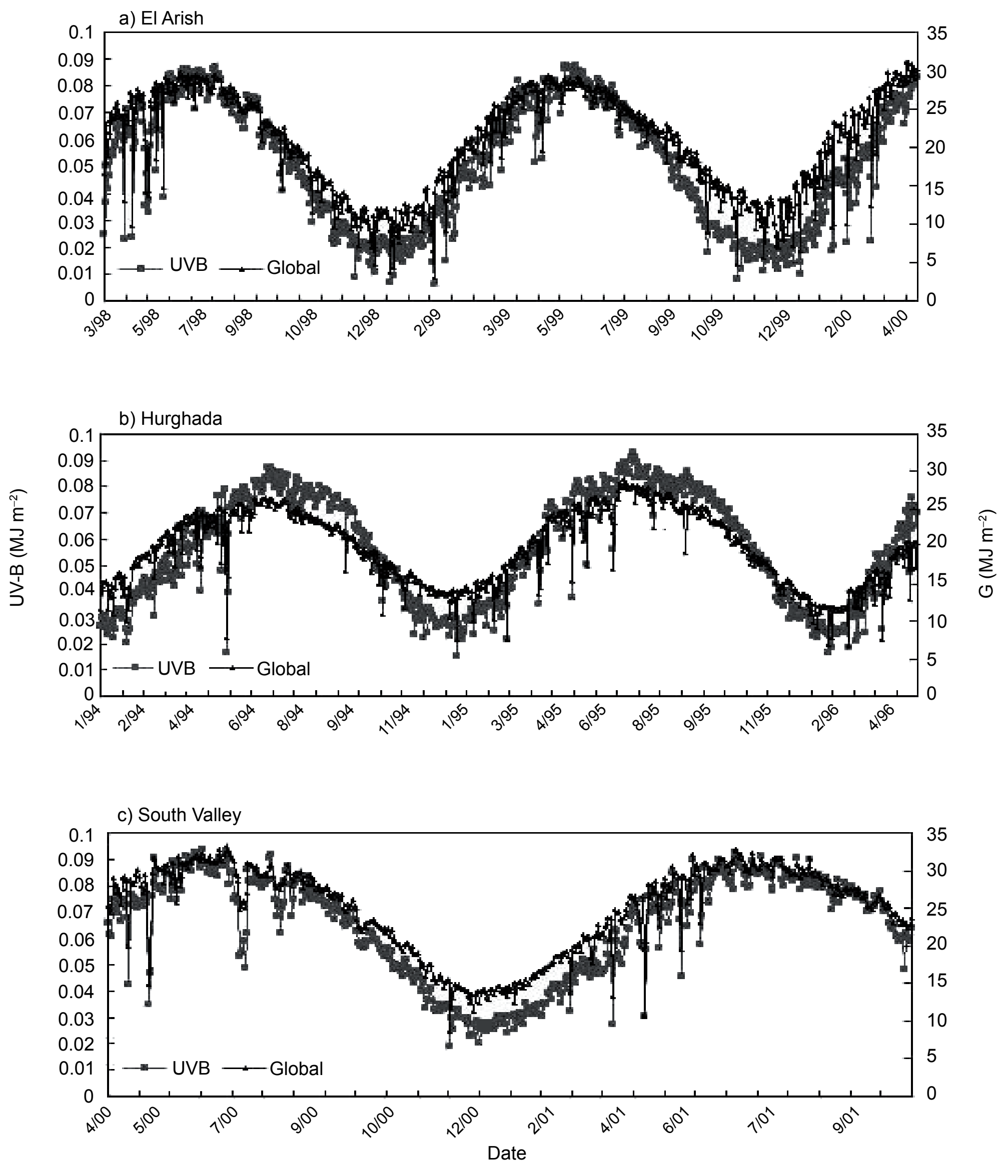

Fig. 1. Daily total measured values of UV-B and global radiation at a) El-Arish from Apr. 1998 to May 2000. b) Hurghada since Jan. 1994 to Apr. 1996. c) South Valley since Apr. 2000 to Sep. 2001. d) Aswan from Aug. 1998 to Dec. 2000. (Continues in the next page).

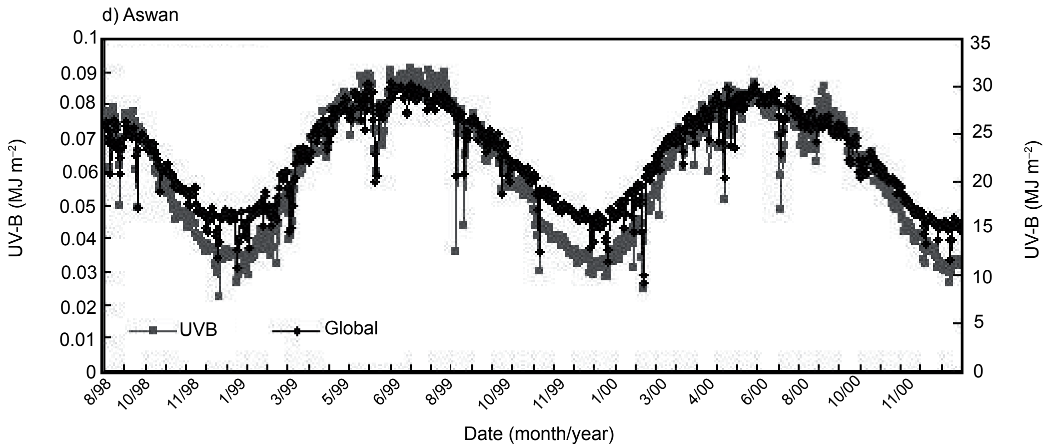

Fig. 1. Daily total measured values of UV-B and global radiation at a) El-Arish from Apr. 1998 to May 2000. b) Hurghada since Jan. 1994 to Apr. 1996. c) South Valley since Apr. 2000 to Sep. 2001. d) Aswan from Aug. 1998 to Dec. 2000. (Continued).

3.1 Empirical equations for estimating UV-B from global radiation

In this section, we will use the strong relationship between G and UV-B illustrated above at our four stations to deduce linear regression equations, relating these two variables at each station. The location and the available data periods of our main four stations are illustrated in Table II. The regression equations that have been deduced using the available daily values of global and UV-B can be written in the following forms:

$$UV\text{-}B_{Arish} = -\,0.01839 + 0.00337 * G_{Arish} \quad (1)$$

$$UV\text{-}B_{Aswan} = -\,0.02333 + 0.00371 * G_{Aswan} \quad (2)$$

$$UV\text{-}B_{Hurghada} = -\,0.01873 + 0.00336 * G_{Hurghada} \quad (3)$$

$$UV\text{-}B_{S.\ Valey} = -\,0.02269 + 0.00398 * G_{S.\ Valley} \quad (4)$$

Table II. The location and the available data period of the main four stations.

WMO No.	Station	Lon. (°E)	Lat. (°N)	Alt. m	Data period
337	El-Arish	33.83	31.08	32	Apr 1998-May 2000
464	Hurghada	33.75	27.28	6.5	Jan 1994-Apr 1996
403	South Valley	32.7	26.18	77.3	Apr 2000-Sep 2001
414	Aswan	32.78	23.97	192	Aug 1998-Dec 2000

3.2 Observed and estimated UV-B

Equations (1) to (4) illustrate the linear regression equations for the four stations. They were applied on the available used data of each station to evaluate their accuracy. Table III shows the regression coefficients, the root mean square error (RMSE), and the mean absolute error (MAE) arising from the error between the measured and estimated values of UV-B for each station. It also shows the available record length and the correlation coefficient (CC) between G and UV-B at each station.

Table III. The regression coefficients, root mean square error (RMSE), the mean absolute error (MAE), and the correlation coefficients (CC) between the actual and estimated values at each station.

Station	Regression coefficients		RMSE	MAE	CC	Record length (days)
	C_0	C_1				
El Arish	–0.01839	0.00337	0.00572	0.00464	0.9684	750
Aswan	–0.02333	0.00376	0.00373	0.00288	0.9789	840
Hurghada	–0.01873	0.00336	0.00584	0.00467	0.9596	730
South Valley	–0.02269	0.00398	0.00358	0.00259	0.9837	520

Figure 2a represents the measured and estimated daily values of UV-B of Hurghada station. It shows the strong correlation between the measured and estimated values, this strong relation can be also noticed from Figure 2b which represents the error between the measured and estimated values of UV-B. The root mean square and the mean absolute values of this error are 0.00584 and 0.00467, respectively. The maximum correlation between the observed and estimated values of UV-B of the four stations occurs at South Valley (Table III). The comparison between the observed and estimated values of UV-B at Aswan is illustrated in Figure 3a, while the error between them is shown in Figure 3b.

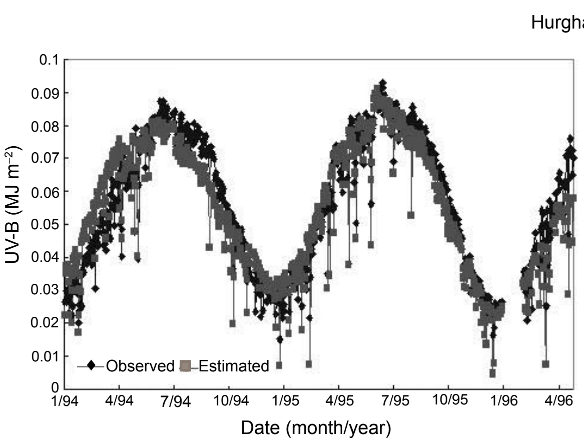

Fig. 2a. Daily observed and estimated UV-B at Hurghada.

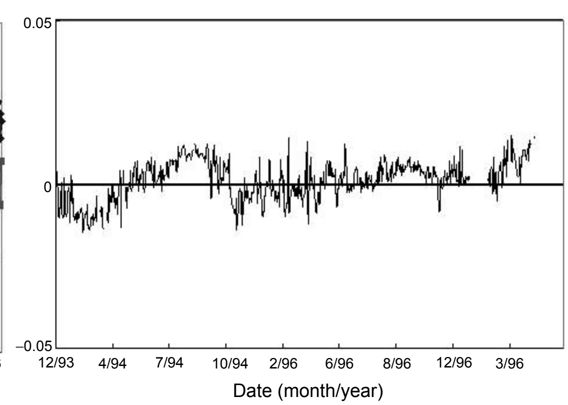

Fig. 2b. Error between observed and estimated UV-B at Hurghada.

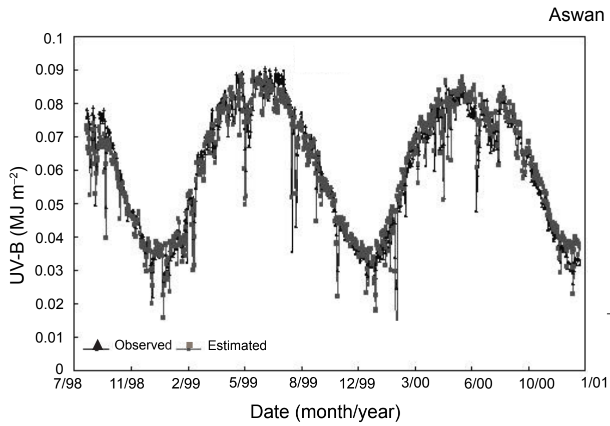

Fig. 3a. Daily observed and estimated UV-B at Aswan.

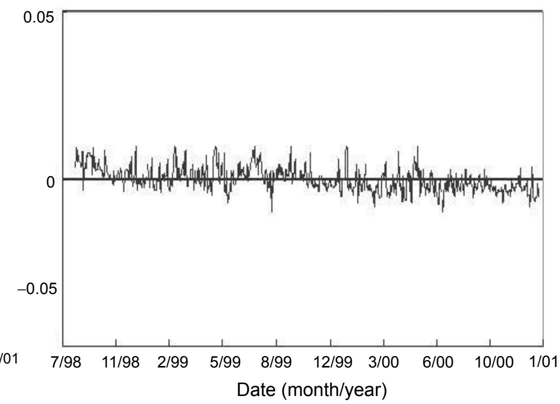

Fig. 3b. Error between observed and estimated UV-B at Aswan.

4. The annual and monthly variation of UV-B over Egypt

In the previous section, we used the strong correlation between G and UV-B radiation to establish empirical formulas that enable us to estimate UV-B from G at each station. These empirical formulas can also be utilized to estimate UV-B for another period where the values of G are available at the same station. Also, it can be utilized to estimate UV-B for other neighboring stations in the same region and having the same geography and climate.

In this section we will use the linear regression equations (1 to 4) to estimate UV-B radiation at other stations where the global solar radiation data are available. We used the regression equation 2 (for Aswan) to estimate the UV-B for the stations El-Kharga, Asyout, Bahtim, Cairo and El-Tahrir. On the other hand the regression equation 1 (for El-Arish) was used as an empirical model for estimating UV-B of the stations Mersa Matruh, Sidi Barani and Rafah. The longest period of continuous measurements of daily global solar radiation was at El-Kharga (26 years) while the shortest was at south valley (2 years).

Figure 4a-c represents the annual variation for all twelve stations. The figures are classified depending on the latitude from south to north for the sake of comparison. The annual variation of the monthly mean values of UV-B at Aswan, El-Kharga, South Valley, and Asyut is illustrated in Figure 4a, while Figure 4b shows the annual variation of Hurghada, Bahtim, Cairo and El-Tahrir.

Finally, Figure 4c illustrates the coastal stations: El-Arish, Rafah, Mersa Matrouh, and Sidi Barani. Figure 4 shows that at all stations the annual cycle of UV-B appears clear with minimum values in the cold months (especially in January and December) and maximum values in the warm months (especially in June). The values of UV-B at the stations that lie in the south of Egypt (Aswan, El-Kharga, South Valley, and Asyut) are higher than those located in the middle and northern Egypt (Bahtim, Cairo, El-Tahrir, El-Arish, Rafah, Mersa Matrouh, and Sidi Barani). Figure 4b represents a good example for the comparison between Upper Egypt (south Egypt) and Lower Egypt (north Egypt) stations, where the values of UV-B throughout the year at Hurghada are greater than those corresponding values at Bahtim, Cairo and El-Tahrir. This is due to the fact that the amount of insulation at Upper Egypt is greater than that at Lower Egypt. Also the amount of pollution over Upper Egypt and Hurghada is smaller than that over Cairo and Lower Egypt.

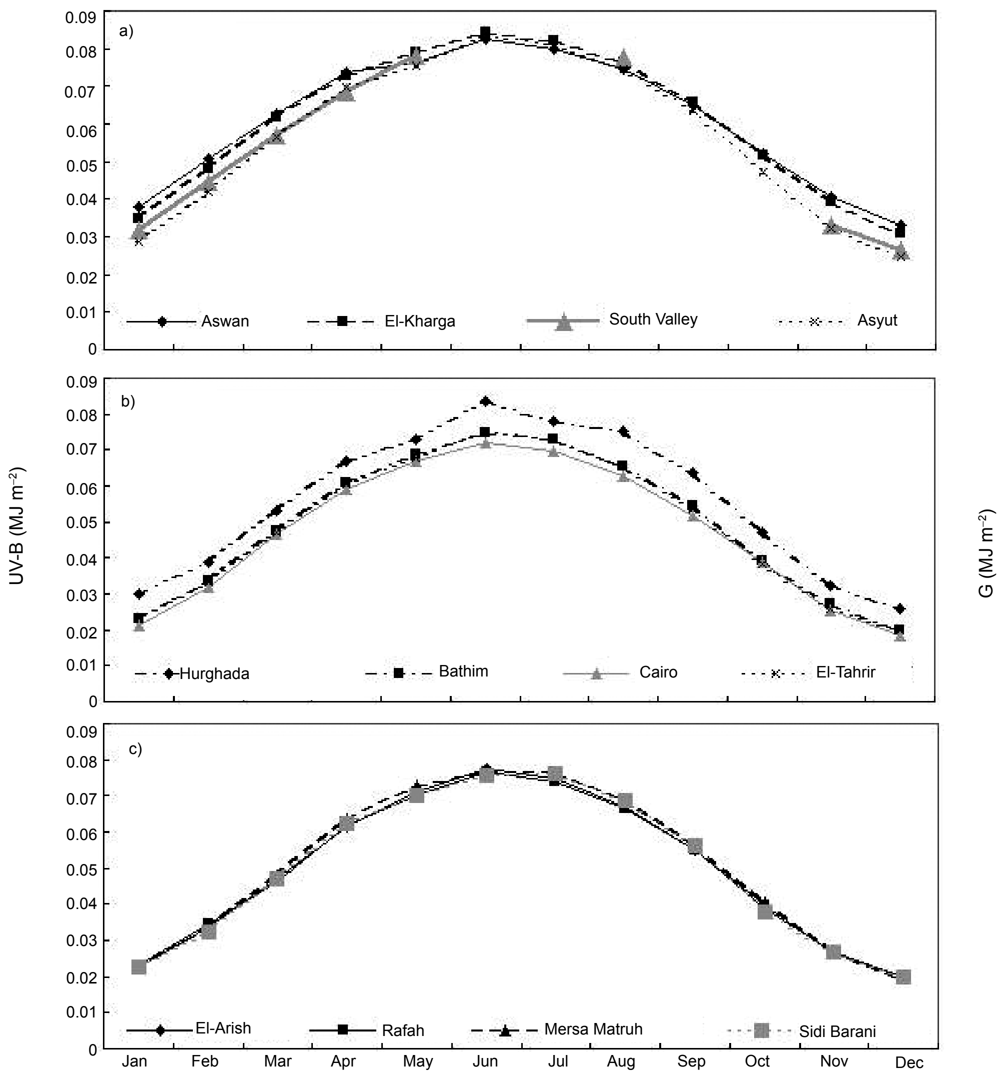

Fig. 4. The annual variation of monthly values of UV-B at a) Aswan, El-Kharga, South Valley and Asyut. b) Hurghada, Bathim, Cairo and Tahrir. c) El-Arish, Rafah, Mersa Matruh and Sidi Barani.

To drive the climatic pattern of UV-B radiation of a region, it is necessary to collect extensive radiation data of high accuracy at a large number of stations covering this region. The radiation network density normally accepted as satisfactory is one that provides a station-to-station spatial correlation of data of at least 0.7 (0.9 is easily achievable in homogeneous regions), for corresponding monthly mean values of daily totals of global solar radiation. It was suggested by Pivovarova (1978) that, except for regions with strong gradients such as coastal and mountainous areas, this requirement is probably reached with stations of 500 km grid. In Egypt there are no large variations in terrain. The stations spacing is not so long, i.e. the network satisfies the above characteristics, so in the absence of actual measurements we can calculate the UV-B radiation from other meteorological parameters or by using empirical models from neighboring stations.

Due to the inadequate number of stations having instruments to measure UV-B in Egypt, use of suitable empirical equations to estimate UV-B from G in the Egyptian network will lead to get useful values of UV-B at these stations for a long period. The monthly mean values of UV-B can be calculated for all available stations having G measurements. Figure 5a, b shows the distribution of the monthly mean values of UV-B over the whole area of Egypt at each month of the year. The study of this figure illustrates that the distribution of UV-B over Egypt is latitudinal, where its intensity tends to increase southward and decrease northward. The monthly mean values of UV-B radiation ranged from a highest value of 0.088 MJ per square meter at the south of Egypt during July to the lowest value of 0.02 MJ per square meter at the north of Egypt during December. There is a marked difference between the intensity of UV-B radiation at the north and south part of Egypt especially during late autumn, winter and early spring. On the other hand there are permanent low values of UV-B over the urban area of Cairo and Nile Delta as a result of the marked increase of man activity and high pollution concentration.

5. Harmonic analysis of erythemal UV-B

5.1 Data

The erythemal exposure data product is an estimate of the daily-integrated ultraviolet irradiance, calculated using a model for the susceptibility of Caucasian skin to sun burn. This can be interpreted as an index of the potential for biological damage due to solar irradiation. These data were archived on regular latitude-longitude grid points with resolution of $1 \times 1.25°$. From this data archive, daily data were used for the period (1998-2001) to study the periodic variation of erythemal UV-B.

5.2 Analysis

The harmonic analysis has been applied to study the variations of the daily and monthly time series of erythemal UV-B of the stations El-Arish, Aswan, Hurghada and South Valley. We deal with record lengths (N, N-1, N-2,…), each time we get the wave with the largest contribution. From these waves we considered the one with minimum root mean square deviation from the actual data as real wave in the record. After subtracting this wave from the actual data, the analysis is repeated again to obtain the next one. We repeated the technique until we get the wave with negligible contribution to the record.

The analysis of UV-B daily values for El- Arish for four years period (1440 values) shows that there is only one dominant wave of 13 months in this time series. It accounts for 96% of the total variance of UV-B with an amplitude of 0.2806E-02. While the analysis of the daily time series of

Aswan shows that there is also one dominant wave. Its length is 13.5 months and its amplitude is 0.2215E-02. Results of the UV-B time series of South Valley and Hurghada illustrate that the dominant wave in these two series is 13.4 months, which accounts for 96% of the total variance in the two series during our study period. The amplitudes of both waves are 0.2441E-02 for the time series of South Valley and 0.251987E-02 for Hurghada. Mean monthly analysis for the four stations shows that the dominant wave in those four time series is the annual wave. It accounts for 99, 95, 98 and 95% of the total variance of El- Arish, Aswan, Hurghada and South Valley time series, respectively, with amplitudes of 0.2688E-02, 0.2053E-02, 0.2382E-02 and 0.2319E-02. Figure 6a-d shows the monthly values of UV-B at our stations during the period of study (solid curve). It is clear that the annual oscillation has the greatest amplitude (the dominant wave). Actual data can be presented successfully by the annual wave of each station, so there is no need to add additional harmonics. Dashed curves represent the calculated annual waves; we extend it as a prediction for 3 years after the actual data. The error between the actual data and the calculated waves is presented below each figure.

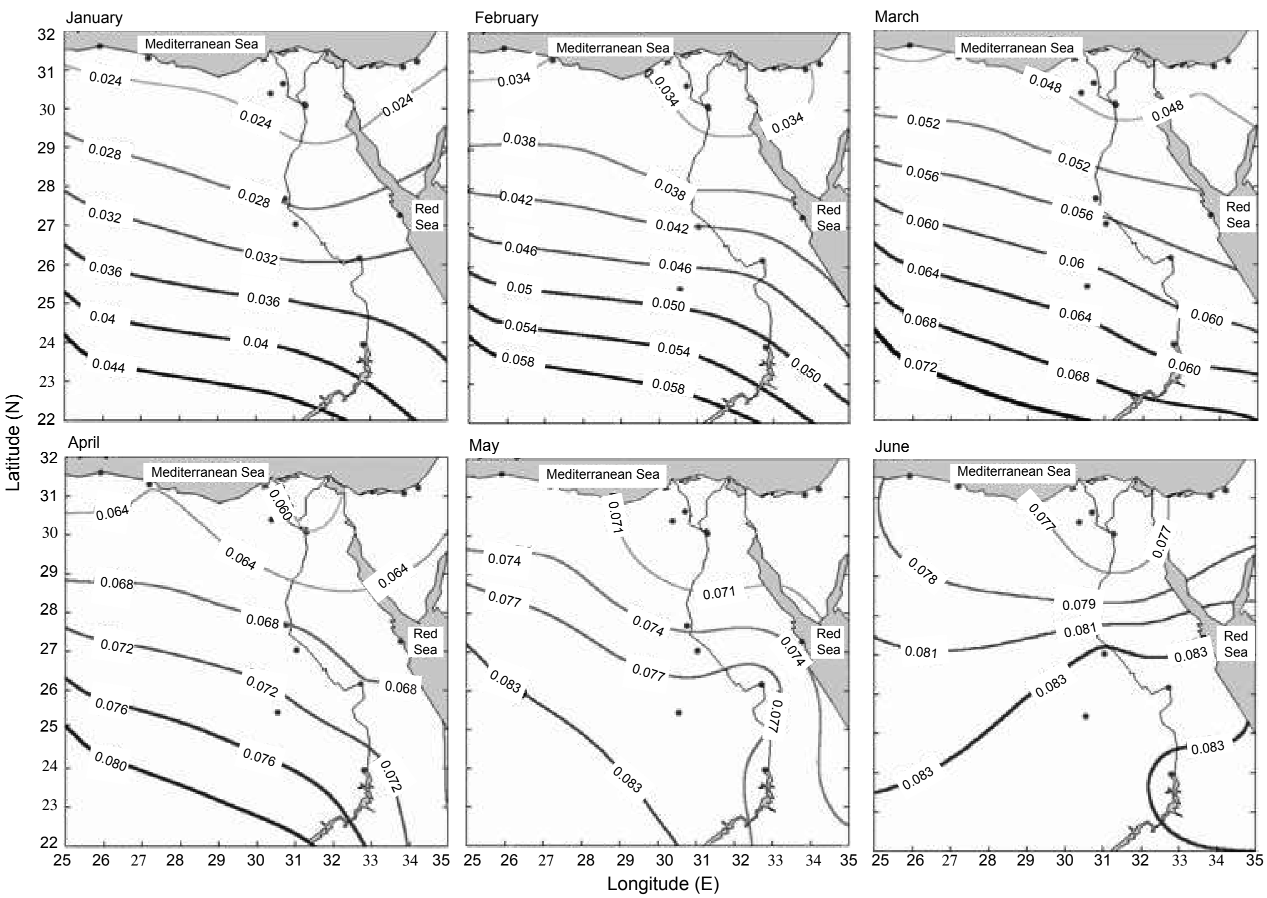

Fig. 5a. The distribution of monthly pattern of UV-B (MJ m^{-2}) over Egypt from January to June.

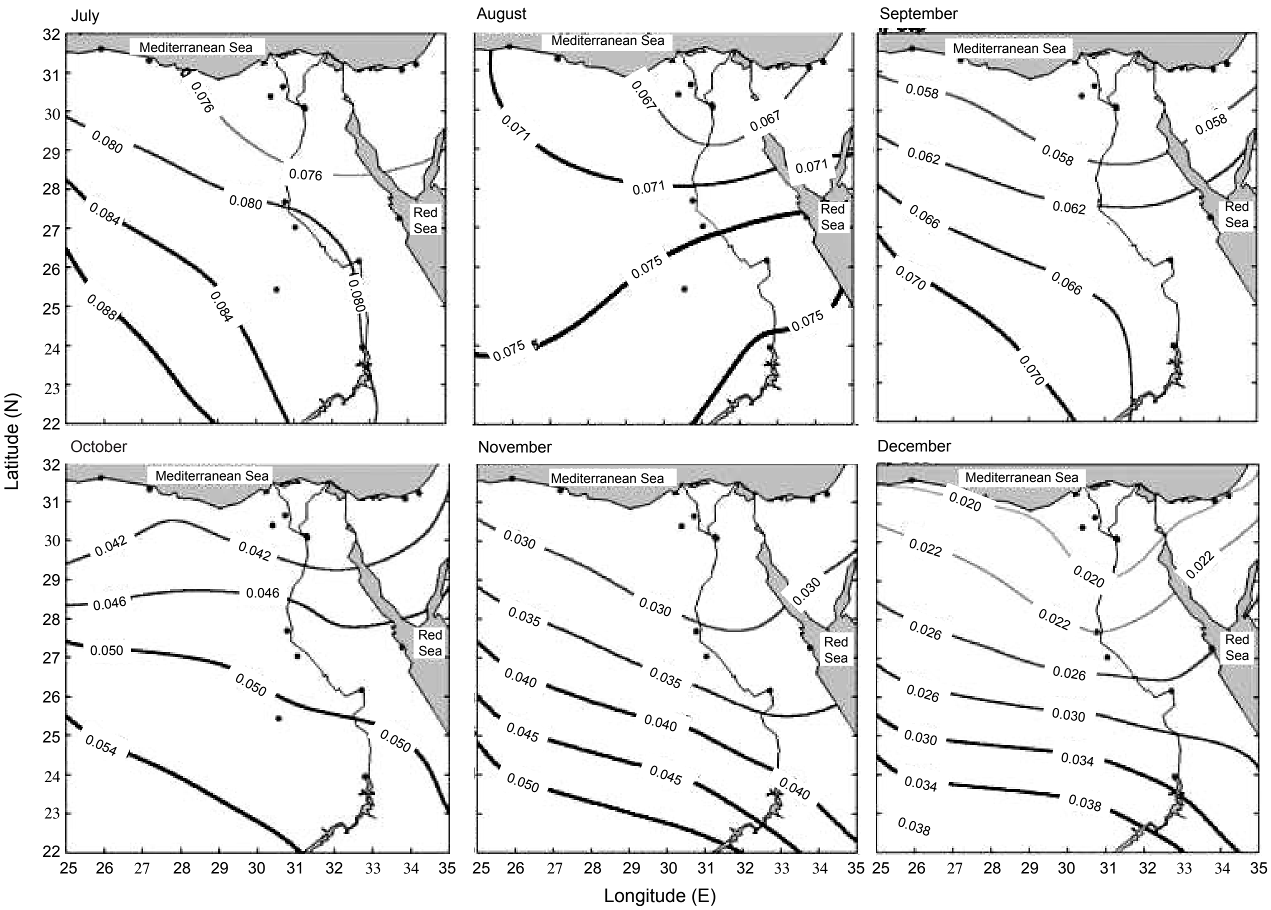

Fig. 5b. The distribution of monthly pattern of UV-B (MJ m^{-2}) over Egypt from July to December.

The dominant waves which appeared during the analysis of the daily time series of the four stations (13, 13.5, 13.4, 13.4 months) seem to be associated with quasi-biennial oscillation. This connection has been mentioned by other researchers. Scherhag (1967) found that quasi-biennial oscillation (QBO) appears to affect the overall mean temperature of the entire (Northern Hemisphere) atmosphere from the surface up to 16 km. The changes in solar UV-B radiation reaching the ground has been documented with QBO affecting clear sky UV solar irradiances at Thessaloniki (Zerefos *et al*., 1998). Udelhofen *et al*. (1999) performed a detailed time series analysis for the Australian continent, based on TOMS erythemal dose observations. They associated changes of UV erythemal exposure to phases of the QBO and the solar activity cycles. Cabrera and Fuenzalida (1999) reported evidence of the QBO in measurements of UV solar irradiance at Santiago, Chile.

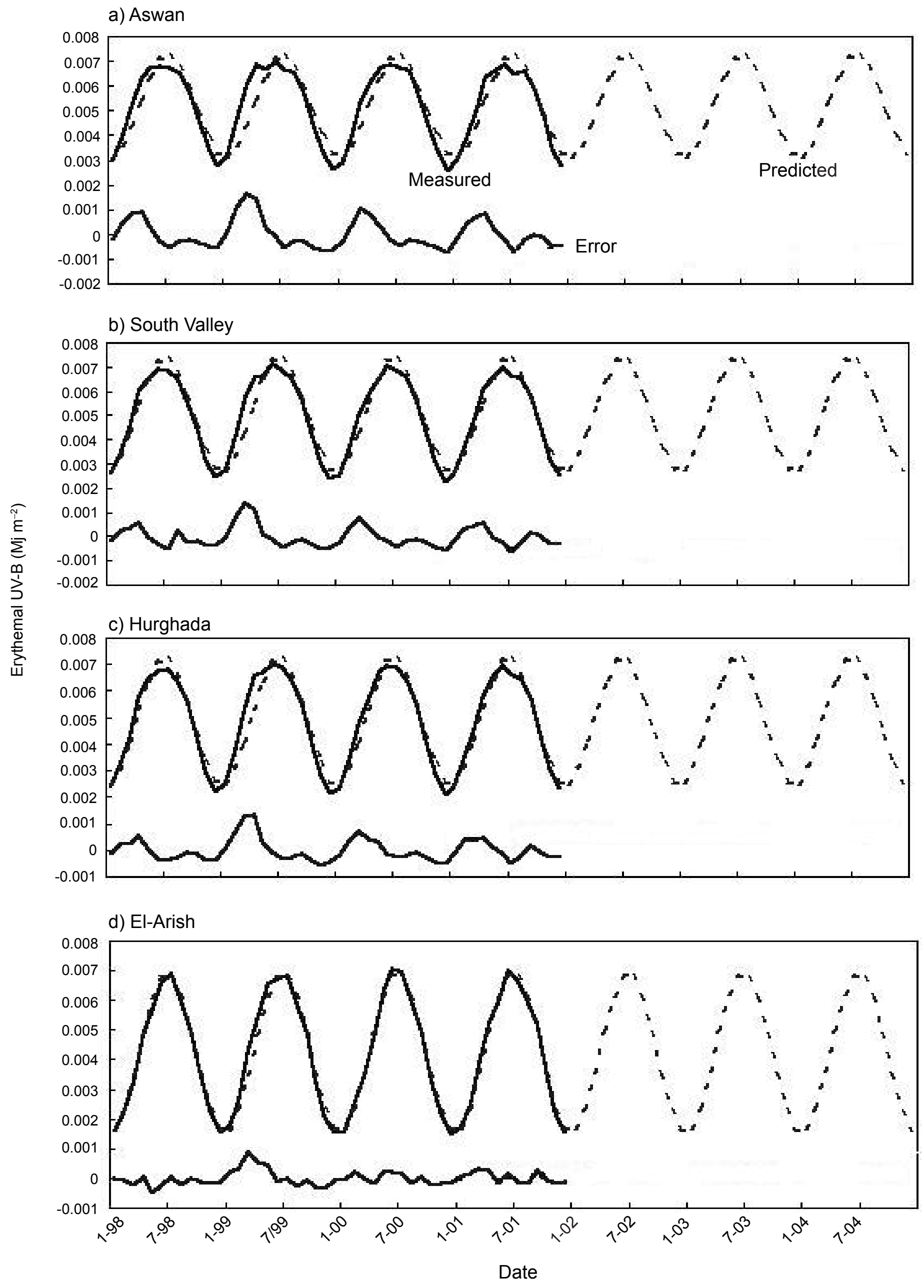

Fig. 6. The monthly mean values of erythemal UV-B (solid curves), the predicted values of erythemal UV-B (dashed curves) and the error between the actual and the predicted values of erythemal UV-B at a) Aswan, b) South Valley, c) Hurghada, d) El-Arish.

The relative importance of the QBO cycle for the amplitude of the annual variation of the UV erythemal dose was examined by calculating the ratio of the QBO amplitude over the amplitude of the annual variation at the same latitude, and for different latitude zones (Zerefos *et al*., 2001). In the tropics the amplitude of the QBO effect is about 40% that of the annual cycle, while at middle latitudes, where Thessaloniki and San Diego are placed, it is only 5%, so it seems to be decreasing with latitude. Therefore (Zerefos *et al*., 2001) conclude that the biologically important erythemal dose reaching ground level at low latitudes has a QBO component which cannot be overlooked, even in comparison with the amplitude of the annual cycle.

6. Estimation of UV-B using Fourier series

The available data of UV-B and G in the four references stations (Aswan, South Valley, Hurghada, El-Arish) were employed together with equations (a7) and (a8) (Appendix) to determine the Fourier coefficients for these stations. These Fourier coefficients were used to calculate the UV-B for the same reference stations by using equation a10. Table IV shows the RMSE and MAE between the observed and calculated values of UV-B. It is clear that there is a close agreement between the measured and calculated UV-B values at the four stations with the smallest value at Hurghada.

Table IV. The RMSE and MAE between the measured and calculated UV-B from Fourier series for the four stations.

Station	RMSE	MAE
El Arish	0.00079	0.00029
Hurghada	0.00026	0.00004
South Valley	0.00028	0.00022
Aswan	0.00056	0.00011

In order to compare between this method and the linear regression method, Fourier coefficients for the stations Aswan and El-Arish have been used to calculate the UV-B at South Valley and Rafah respectively. The comparisons between the two methods are shown in Figures 7b and 8b and the error between the observed and calculated values arising from the two methods at South Valley and Rafah. Figures 7a and 8a show that there is a good agreement between the measured and calculated values of UV-B at both stations. It is clear that the linear regression method is more accurate than the Fourier method due to the fact that the variations of global solar radiation between overcast and clear skies is linear in UV-B radiation, while the estimated values of UV-B from Fourier method are affected only by the arising waves from the available data.

Also, the comparison between the error arising from the two methods at the four main stations and at Rafah and South valley illustrate that:

- The magnitude of RMSE and MAE between the calculated and measured UV-B at the main four stations from linear regression method is greater than the corresponding from the Fourier series method (Table III and IV).

- The magnitude of RMSE and MAE between the calculated and measured UV-B at Rafah and South Valley stations from Fourier series method is greater than the corresponding from the linear regression method (Table V).

Table V. The RMSE and MAE between the measured and calculated UV-B from the two methods.

Station	Linear regression		Fourier series	
	RMSE	MAE	RMSE	MAE
Rafah	0.00374	0.002973	0.010274	0.009173
South Valley	0.00551245	0.004331	0.010726	0.009346

The above results indicate that Fourier method is better than linear regression method in case of estimating UV-B at the same station, while the linear regression method is better in case of estimating UV-B at a neighboring station.

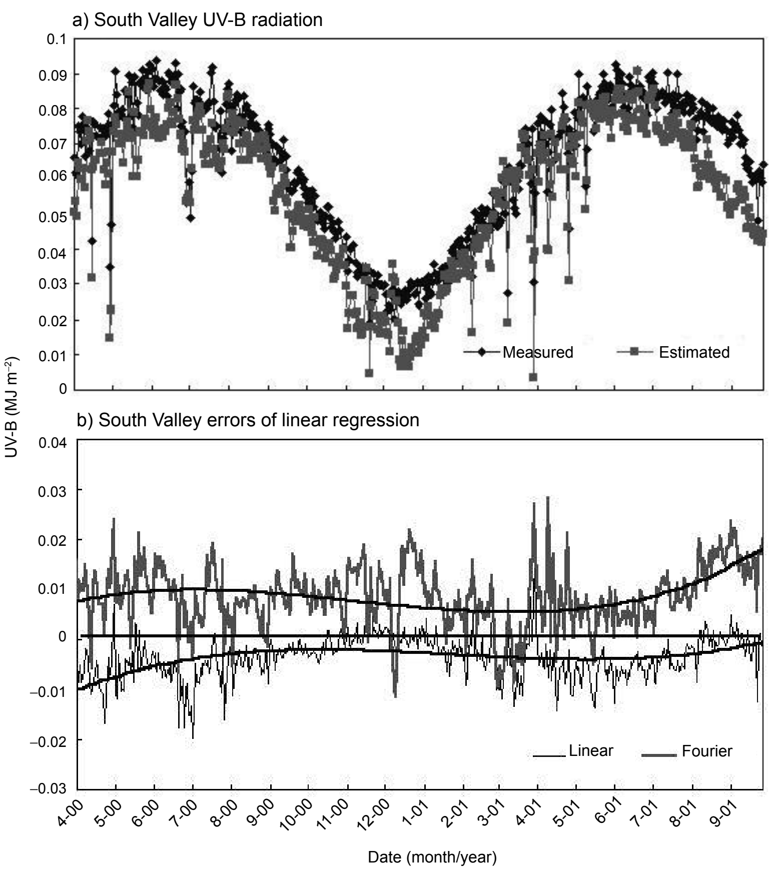

Fig. 7. a) The measured and estimated UV-B using Fourier series at South Valley. b) The comparison between the linear regression error and Fourier series error of the estimated values of UV-B estimation at South Valley.

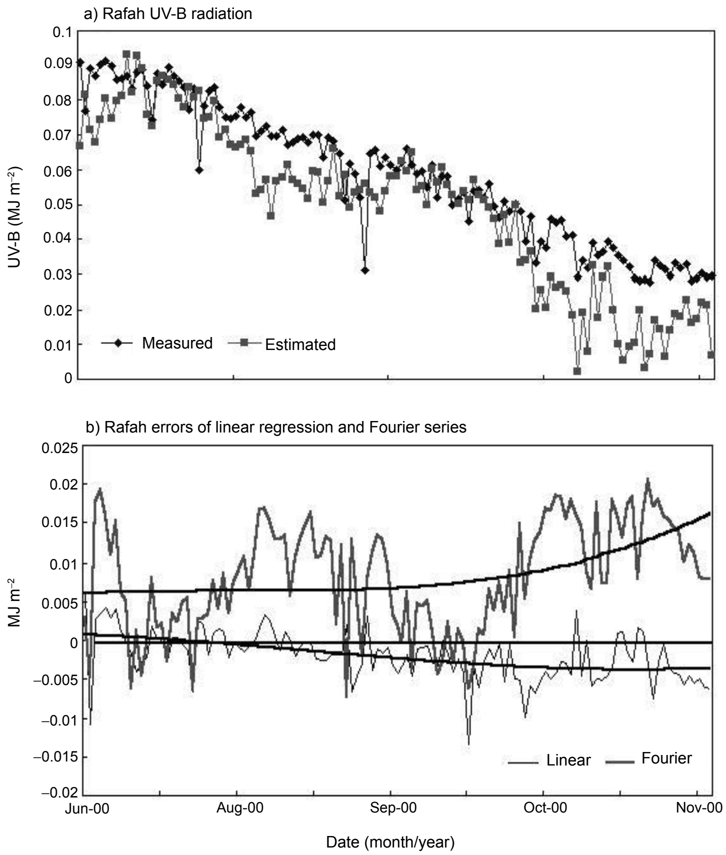

Fig. 8. a) The measured and estimated UV-B using Fourier series at Rafah. b) The comparison between the linear regression error and Fourier series error of the estimated values of UV-B at Rafah.

7. Conclusions

The relationships between the global solar radiation and UV-B radiation at four stations of Egypt have been studied. We deduced linear empirical formulas for estimating UV-B from global radiation at these stations. The deduced equations were applied to calculate the UV-B radiation for other stations where UV-B radiation measurements were unavailable, using records of global radiation at these stations.

Periodicities of the daily and mean monthly values of erythemal UV-B of the stations El-Arish, Aswan, Hurghada and South Valley have been examined. The harmonic analysis has been applied to study the variations of the daily and monthly time series of erythemal UVB of these four stations. It was found that the dominant wave that appeared with the analysis of the daily time series of the four stations was 13 (El-Arish), 13.5 (Aswan) 13.4 (Hurghada) and 13.4 (South Valley) months. The analysis of the mean monthly values for the four stations showed that the dominant wave in these four time series was the annual wave with high statistically significant results. These annual waves were used in forecasting UV-B for these stations.

Because of the periodicity of variations in solar radiation, global and UV-B radiation, their non-dimensional values are expanded in Fourier series. Fourier coefficients were determined by using measured global solar radiation data for the four selected Egyptian weather stations. These coefficients were used to calculate UV-B radiation based on global solar radiation for the same stations. A comparison between the observed and calculated UV-B radiation showed a good agreement. The method can also be applied to calculate the UV-B radiation for other neighboring stations where UV-B radiation measurements are unavailable. This can be done by using records of global solar radiation at these stations. The method is an excellent technique, which can be used when the required meteorological data are not available.

The comparison between the two methods illustrated that Fourier method is better than linear regression method in case of estimating UV-B at the same station, while the linear regression method is better in case of estimating UV-B at a neighboring station using records of global solar radiation.

Appendix. Analysis of UV-B using Fourier series

We present a theoretical method to calculate daily values of UV-B based on global radiation. The dimensionless values of global solar radiation (G), UV-B radiation (UV-B) can be written as (Hussain, 1992).

$$[UV\text{-}B]\,\frac{UV\text{-}B - UV\text{-}B_{\min}}{UV\text{-}B_{\max} - UV\text{-}B_{\min}} \tag{a1}$$

$$[G] = \frac{G - G_{\min}}{G_{\max} - G_{\min}} \tag{a2}$$

Where the subscript "min", "max" indicates the minimum and maximum values of UV-B and G for a complete year. The daily values of UV-B and G are represented graphically during the available period of the stations El-Arish (Apr. 1998 to May 2000), Hurghada (Jan. 1994 to Apr. 1996) South Valley (Apr. 2000 to Sep. 2001) and Aswan (Aug. 1998 to Dec. 2000), as shown in (Fig. 2b). The graph indicates the periodicity of the variations of the values of UV-B and G at our selected stations, therefore the dimensionless values of UV-B radiation and global solar radiation could be expanded in Fourier series as follows:

$$UV\text{-}B_N = \frac{A_{0UVB}}{2} + \sum_{j=1}^{\infty}\left[A_{UVB_j}\cos\frac{\pi\, j N}{m} + B_{UVB_j}\sin\frac{\pi\, j N}{m}\right] \tag{a3}$$

$$G_N = \frac{A_{0G}}{2} + \sum_{j=1}^{\infty}\left[A_{G\,j}\cos\frac{\pi\, jN}{m} B_{G\,j}\sin\frac{\pi\, jN}{m}\right] \tag{a4}$$

Where N is the number of days (record length), and m = N/2.

Subtracting equation (a4) from equation (a3) we obtain:

$$UV\text{-}B_N - G_N = \frac{A_0}{2} + \sum_{j=1}^{\infty} \left[A_j \cos\frac{\pi\, jN}{m} + B_j \sin\frac{\pi\, jN}{m} \right] \tag{a5}$$

Where

$$A_0 = \frac{A_{0UVB} - A_{0G}}{2} \tag{a6}$$

After simple mathematical treatment, we can obtain the following expression for the Fourier coefficients:

$$A_j = A_{UVB\,j} - A_{G\,j} = \frac{2}{N}\sum_{i=1}^{N}\left(UV\text{-}B_i - G_i\right)\cos\frac{\pi\, ji}{m}, \left(j = 0, 1, 2, \ldots\right) \tag{a7}$$

and

$$B_j = B_{UVB\,j} - B_{G\,j} = \frac{2}{N}\sum_{i=1}^{N}\left(UV\text{-}B_i - G_i\right)\sin\frac{\pi\, ji}{m}, \left(j = 1, 2, 3, \ldots\right) \tag{a8}$$

Where the summation in these equations extends over the number of observations N. By using equation (a6), equation (a1) can be written as:

$$UV\text{-}B = UV\text{-}B_{\min} + (UV\text{-}B_{\max} - UV\text{-}B_{\min})\left(G_N + \frac{A_0}{2} + \sum_{j=1}^{\infty} \left[A_j \cos\frac{\pi\, jN}{m} + B_j \sin\frac{\pi\, jN}{m} \right]\right) \tag{a9}$$

Kenisarin and Tkachenkova (1992) found that for the number of observations N, the number of harmonics that describe the variation of the periodic function *($UV\text{-}B_N - G_N$)* sufficiently well equal N/2. Since we are dealing with the daily sum values of UV-B radiation and global solar radiation, then the sum in (a9) of the Fourier series can be written as:

$$UV\text{-}B = UV\text{-}B_{\min} + (UV\text{-}B_{\max} - UV\text{-}B_{\min})\left(G_N + \frac{A_0}{2} + \sum_{j=1}^{m} \left[A_j \cos\frac{\pi\, jN}{m} + B_j \sin\frac{\pi\, jN}{m} \right]\right) \tag{a10}$$

Equation (a10) enables us to calculate UV-B radiation as a function of global solar radiation in a specific geographic location by using available global radiation data measured at weather stations.

References

(ASTM), 1981. Standard solar constant and air mass zero solar spectral irradiance tables. ASTM standard E490-73a, (heapproved 1992). American Society for Testing and Materials.

Cabrera S. and H. A. Fuenzalida, 1999. Interannual variation of global UV radiation in Santiago, Chile(33.5S), *Geophys. Res. Lett*. **26**, 2945-2948.

Frederick J. E. and E. Carynelisa, 1994. The ultraviolet radiation of the biosphere, WMO, Global Atmospheric Watch No.100, ANNEX D.

Hussain H., 1992. Correlating beam radiation with sunshine duration. *Solar Energy* **48**, 145-149.

Ilyas M., A. Pandy and S. I. S. Hassan, 1999. UV-B radiation at Penang, *Atmospheric Research* **51**, 141-152.

Iqbal M., 1983. *An introduction to solar radiation*. Academic Press, New York, 390 pp.

Kenisarin M. M. and N. P. Tkachenkova, 1992. Estimation of solar radiation from ambient air temperature. *Applied Solar Energy* **28**, 63-57.

Koronakis P. S., G. K. Sfantos, A. G. Paliatsos, J. K. Kaldellis, J. E. Garofalakis and I. P. Koronaki, 2002. Interrelations of UV-global/global/diffuse solar irradiance components and UV-global attenuation on air pollution episode days in Athens, Greece. *Atmospheric Environment* **36**, 3173-3181.

Pivovarova Z. I., 1978. On the accuracy of solar radiation data, network observations and network density. Unpublished presentation, World Meteorological Organization, Geneva.

Udelhofen P., P. Gies, C. Roy and W. J. Randel, 1999. Surface UV radiation over Australia, 1979-1992: effects of ozone and cloud cover changes on variations of UV radiation. *J. Geophys. Res*. **104**,19135-19159.

Zerefos C. S., C. Meleti, D. Balis, K. Tourpali and A. F. Bais, 1998. Quasi-biennial and longer term changes in clear sky UV-B solar irradiance. *Geophys. Res. Lett*. **25**, 4345-4348.

Zerefos C. S., D. Balis, M. Tzortziou, A. Bais, K. Tourpali, C. Meleti, G. Bernhard and J. Herman, 2001. A note on the interannual variation of UV-B erythemal doses and solar irradiance from ground-based and satellite observations. *Annales Geophysicae* **19**,115-120.